A unified mechanism for oxidative coupling and partial oxidation of methane

Yves Simon, Paul-Marie Marquaire

A unified mechanism for oxidative coupling and partial oxidation of methane

Yves Simon*, Paul-Marie Marquaire

Université de Lorraine, CNRS-Laboratoire Réactions et Génie des Procédés (UMR7274),

ENSIC, 1 rue Grandville, BP 20451, F-54001 Nancy Cedex, France

* Corresponding author. E-mail address: yves.simon@univ-lorraine.fr

ABSTRACT

The oxidative coupling (OCM) and the partial catalytic oxidation (POM) of methane as well as the homogeneous oxidation of methane (HOM) differ only in the ratio CH_4 / O_2 used and of course in the use of a catalyst. It can therefore be considered that their overall reaction mechanism should be the same with elementary reactions of varying importance depending on the type of oxidation reaction studied. We have therefore tried to represent the results obtained during the experimental study of OCM and POM over La_2O_3 and that of the oxidation of methane in gas phase from a single mechanism. At high temperature, OCM and POM are catalytic reactions but their reaction mechanisms are very complex because the surface reactions are coupled to reactions in gas phase by the intermediary of radicals, so both homogeneous and heterogeneous mechanisms occur at the same time. In this work, the development and the validation of a hetero-homogeneous mechanism is proposed for the three reactions. This mechanism is based on elementary steps at the catalyst surface and elementary steps in gas phase for a large range of temperature (973K – 1173K) and residence time (0.7s – 5.5s).

Keywords: Methane; kinetic mechanism; partial oxidation; oxidative coupling; La_2O_3.

1. INTRODUCTION

Fluctuating prices of fossil fuel and discovery of new natural gas deposits are increasing interest in the upgrading of methane to value-added products. To date, the world reserve of natural gas is estimated about 198.8 trillion cubic meters [1] with steadily increasing in the future. Furthermore, over the past decade, increased production of shale gas has stimulated renewed interest to converting methane into valuable chemicals or liquid fuels.

The oxidative coupling of methane (OCM), first proposed by Keller and Bhasin [2] in 1982, is a direct method of converting methane into higher hydrocarbons especially ethylene. Ethylene is a critical intermediate in the petrochemical industry witch is currently produced by steam cracking of hydrocarbon, mainly ethane. It is a highly endothermic reaction that occurs at high-temperature. Unlike steam cracking, the oxidative coupling of methane is exothermic and allows the direct conversion of methane into ethylene at a lower energy cost compared to current indirect industrial processes. During the 1990s, many studies were devoted to the OCM reaction. These studies showed that the yield of the reaction was not really compatible with an industrial application. However, in the last few years, the interest in the OCM reaction has increased because catalysts with higher activity and selectivity have been found. Indeed, with oxides as La_2O_3 acceptable reaction performances have been reached [3].

Another way of methane valorisation is the catalytic partial oxidation (POM). The catalytic partial oxidation of methane is an alternative to steam reforming [4, 5] for synthesis gas ($CO + H_2$) production. One advantage of POM is the production of syngas [6-8] with a H_2/CO ratio ideal for a subsequent Fischer–Tropsch synthesis. In contrast to steam reforming, the partial oxidation is an exothermic reaction and therefore requires a smaller amount of heat energy. Furthermore, POM has a good dynamic response time and could therefore be used as an on-board hydrogen generator for fuel cells.

OCM and POM are catalytic reactions at high temperatures. Their reaction mechanisms are very complex because the surface reactions are coupled to reactions in gas phase by the intermediary of radicals [9-17], so both homogeneous and heterogeneous mechanisms occur at the same time. Indeed, the general oxidation mechanism includes two sub-mechanisms, one that is related to gas-phase and another that contains the catalytic reactions. Obviously, the homogeneous oxidation of methane (HOM) requires only the gas-phase mechanism. The modelling of the reaction by a detailed mechanism (composed of elementary steps describing the reaction as it occurs at the molecular level) has a lot of advantages. The mechanism and the kinetic analysis results allow a better understanding of the reaction. Indeed, based on this analysis, the reaction pathways, the importance of heterogeneous and homogeneous reactions and the limitative steps can be identified. Since 1982, the literature concerning the study of hetero-homogeneous reactions has been abundant [18,19]. However, there are few detailed mechanisms and much less kinetic data of surface reactions that were published.

The OCM and POM reactions differ only in the ratio CH_4 / O_2 used, so their overall reaction mechanism should be the same. We have therefore tried to represent the results obtained during the experimental study of OCM and POM over La_2O_3 and that of the oxidation of methane in gas phase [20-23] from a single mechanism. The development and the validation of a hetero-homogeneous mechanism is proposed for the three reactions, based on elementary steps at the catalyst surface and on a homogeneous mechanism in gas phase for a large range of temperature and residence time. The experimental study was carried out in a perfectly stirred reactor in presence of lanthanum oxide. The simulations were done by using the Chemkin® software packages.

2. EXPERIMENTAL SECTION

The experimental setup was already described in previous articles (21, 23).

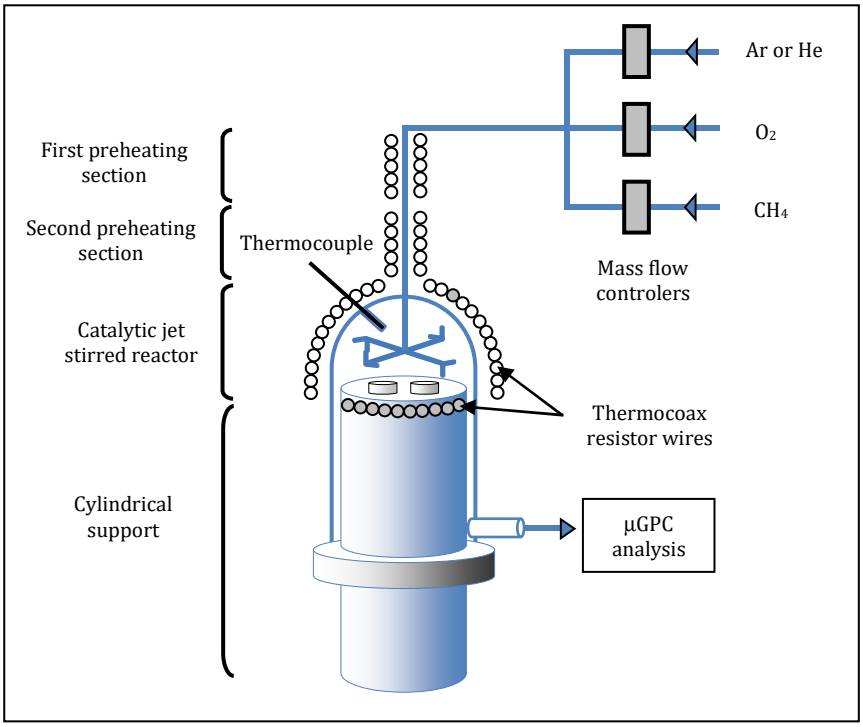

Fig.1. Schematic representation of the catalytic jet-stirred reactor

The reactor developed for the investigation of hetero-homogeneous reactions [24-25] is a continuous stirred tank reactor (CSTR) presented in Fig.1. It consists of two parts: an important well-stirred gas-phase volume (110 cm^3) in contact with catalysts pellets laid on a removable cylindrical support. Four Thermocoax resistance wires that are in contact with the wall are used for heating the reactor. Before entering the reactor, the reactant mixture is preheated. The temperature of the first preheating part is 100°C lower than the reactor temperature while the temperature of the second preheating part equals the one of the reactor. The temperature of the gas phase is measured thanks to a thermocouple located inside a quartz finger at the middle of the free volume.

The catalyst used was Lanthanum oxide. The powder of La_2O_3 was pelleted at a pressure of 20 kN into a cylindrical shape thanks to an electromechanical press Instron 5569.

The pellets are 12 mm wide (diameter) and 1 mm thick. In order to facilitate the desorption of water and also to decompose the carbonates present on the surface of the pellets, the La_2O_3 powder was heated for 8 hours at a temperature of 900 ° C. The BET surface areas are 1,8 $m^2.g^{-1}$ for catalyst pellets used in OCM and 5 $m^2.g^{-1}$ for pellets used in POM.

The outlet gases H_2, CO, CH_4, C_2H_4, C_2H_6 and CO_2 are analysed in line or off line by gas phase chromatography [21 and 23]. Several standard bottles, containing a gas mixture at different concentrations, externally calibrate the chromatograph. All data were collected at a steady state regime and each test was repeated at least three times to verify the stability and repeatability of the measurements.

The experimental conditions used for this study are:

- Temperatures between 973K and 1173K
- Outlet pressure fixed at 1 atm.
- Composition of the gas inlet with $CH_4/O_2 = 5$ for OCM and $CH_4/O_2 = 2$ for POM and HOM.

The reactants are highly diluted in argon or helium (94 % in OCM and 84% in POM or HOM) to better control the reaction temperature and to avoid hot spots.

3. KINETIC MODELING

3.1. Homogeneous mechanism

The mechanism used for simulation includes a heterogeneous part and a homogeneous one. The homogeneous part is described by a set of over 450 elementary reactions. Due to its size, the mechanism cannot be fully presented here; we give only the most significant reactions in Table 1.

	Reactions	A (mol, cm^3, s)	n	E_a (cal. mol^{-1})
1	$O_2 + H = OH + O$	$1.5\ 10^{14}$	0.0	14810
2	$O_2 + H\ (+M) = HO_2\ (+M)$	$4.52\ 10^{13}$	0.0	0.0
3	$O_2 + CHO = CO + HO_2$	$2.6\ 10^{11}$	0.0	410
4	$O_2 + CH_3 = CH_3O + O$	$1.6\ 10^{13}$	0.0	31300
5	$O_2 + HCHO = CHO + HO_2$	$2.0\ 10^{13}$	0.0	38800
6	$O_2 + CH_3 = HCHO + OH$	$3.0\ 10^{30}$	-4.69	36600
7	$O_2 + CH_4 = CH_3 + HO_2$	$4.0\ 10^{13}$	0.0	56700
8	$O_2 + C_2H_5 = C_2H_4 + HO_2$	$8.4\ 10^{11}$	0.0	3900
9	$O_2 + C_2H_3 = HCHO + CHO$	$4.5\ 10^{16}$	-1.39	1000
10	$O_2 + C_2H_3 = C_2H_2 + HO_2$	$1.34\ 10^{6}$	1.61	-400
11	$O_2 + C_2H_2 = 2\ CHO$	$7.0\ 10^{8}$	1.8	30600
12	$O + H_2 = OH + H$	$5.1\ 10^{4}$	2.67	6200
13	$O + CH_3 = HCHO + H$	$8.4\ 10^{13}$	0.0	0
14	$O + CH_4 = CH_3 + OH$	$7.2\ 10^{8}$	1.56	8400
15	$O + C_2H_6 = C_2H_5 + OH$	$1.0\ 10^{9}$	1.5	5800
16	$O + C_2H_4 = CH_3 + CHO$	$8.1\ 10^{6}$	1.88	200
17	$O + C_2H_4 = HCHO + CH_2$	$4.0\ 10^{5}$	1.88	200
18	$O + C_2H_4 = CH_2CO + H_2$	$6.6\ 10^{5}$	1.88	200
19	$O + C_2H_4 = CH_2CHO + H$	$4.7\ 10^{6}$	1.88	200
20	$O + C_2H_4 = OH + C_2H_3$	$1.5\ 10^{7}$	1.91	3700
21	$O + HCHO = CHO + OH$	$4.1\ 10^{11}$	0.57	2700
22	$OH + H_2 = H + H_2O$	$1.0\ 10^{8}$	1.6	3300
23	$OH + CH_3\ (+M) = CH_3OH\ (+M)$	$6.0\ 10^{13}$	0.0	0
24	$OH + CH_4 = CH_3 + H_2O$	$1.6\ 10^{7}$	1.83	2700
25	$OH + CO = CO_2 + H$	$6.3\ 10^{6}$	1.5	-500
26	$OH + HCHO = CHO + H_2O$	$3.4\ 10^{9}$	1.18	-400
27	$OH + C_2H_4 = C_2H_3 + H_2O$	$2.0\ 10^{13}$	0.0	5900
28	$OH + C_2H_4 = CH_3 + HCHO$	$2.0\ 10^{12}$	0.0	900
29	$OH + C_2H_6 = C_2H_5 + H_2O$	$7.2\ 10^{6}$	2.0	900
30	$2\ HO_2 = H_2O_2 + O_2$	$4.2\ 10^{14}$	0.0	11980
31	$HO_2 + H = 2\ OH$	$1.7\ 10^{14}$	0.0	900
32	$HO_2 + CH_3 = CH_3O + OH$	$1.8\ 10^{13}$	0.0	0
33	$HO_2 + CH_4 = CH_3 + H_2O_2$	$9.0\ 10^{12}$	0.0	24600
34	$HO_2 + CO = CO_2 + OH$	$1.5\ 10^{15}$	0.0	23600
35	$HO_2 + CHO = OH + H + CO_2$	$3.0\ 10^{13}$	0.0	0
36	$HO_2 + HCHO = CHO + H_2O_2$	$3.0\ 10^{12}$	0.0	13000
37	$HO_2 + C_2H_6 = C_2H_5 + H_2O_2$	$1.3\ 10^{13}$	0.0	20400
38	$2\ CH_3\ (+M) = C_2H_6\ (+M)$	$3.6\ 10^{13}$	0.0	0.0
39	$2\ CH_3 = C_2H_5 + H$	$3.0\ 10^{13}$	0.0	13500
40	$2CH_3 = C_2H_4 + H_2$	$2.1\ 10^{14}$	0.0	19300
41	$CH_3 + H\ (+M) = CH_4\ (+M)$	$1.7\ 10^{14}$	0.0	0.0
42	$CH_3 + HCHO = CHO + CH_4$	$7.7\ 10^{-8}$	6.1	1970
43	$CH_4 + H = CH_3 + H_2$	$1.3\ 10^{4}$	3.0	8000
44	$C_2H_2 + H\ (+M) = C_2H_3\ (+M)$	$8.4\ 10^{12}$	0.0	2610
45	$C_2H_3\ (+M) = C_2H_2 + H$	$2.0\ 10^{14}$	0.0	39800
46	$C_2H_4\ (+\ M) = C_2H_2 + H_2\ (+\ M)$	$1.0\ 10^{17}$	0.0	71600
47	$C_2H_4 + H = C_2H_3 + H_2$	$5.1\ 10^{7}$	1.93	12900
48	$C_2H_4 + CH_3 = CH_4 + C_2H_3$	$6.3\ 10^{11}$	0.0	1600
49	$C_2H_4 + CH_3 = C_3H_7$	$2.1\ 10^{10}$	0.0	7350

50	C_2H_5 (+M) = C_2H_4 + H (+M)	$8.2\ 10^{13}$	0.0	40000
51	C_2H_6 (+ M) = C_2H_4 + H_2 (+ M)	$2.3\ 10^{17}$	0.0	67400
52	C_2H_6 + H = C_2H_5 + H_2	$1.4\ 10^{9}$	1.5	7400
53	C_2H_6 + CH_3 = C_2H_5 + CH_4	$1.5\ 10^{-7}$	6.0	5800
54	C_2H_6 (+M) = 2CH_3 + (M)	$1.8\ 10^{21}$	-1.24	90900
55	CHO (+ M) = H + CO (+M)	$1.6\ 10^{14}$	0.0	15700
56	CHO + CH_3 = CH_4 + CO	$1.2\ 10^{14}$	0.0	0.0
58	HCHO + H = CHO + H_2	$1.3\ 10^{8}$	1.62	3100
59	CH_2CO (+M) = CH_2 + CO + (M)	$6.57\ 10^{15}$	0.0	57600
60	CH_2CO + H = CH_3 + CO	$1.8\ 10^{13}$	0.0	3400
61	CH_3O_2 = HCHO + OH	$1.5\ 10^{13}$	0.0	47000
62	CH_3O_2 + CH_4 = CH_3O_2H + CH_3	$1.8\ 10^{11}$	0.0	18500
63	CH_3O_2 + CH_3 = 2 CH_3O	$5.0\ 10^{12}$	0.0	-1400

Table 1. Adjusted kinetic parameters of most important homogeneous reactions in oxidation of methane.
$k=A(T)^n\exp(-E/RT)$

The homogeneous mechanism takes into account all elementary reactions between molecules and radicals including less than three carbon atoms. This gas-phase mechanism is well known and has been confirmed by a vast amount of experimental data for different hydrocarbon reactions for the homogeneous oxidation of methane [20; 23; 26].

This mechanism was generated by EXGAS software [27]. In the present work, this mechanism is used in combination with a heterogeneous mechanism for the simulation of the catalytic oxidation of methane reactions.

3.2. Heterogeneous mechanism

3.2.1. Description of the mechanism

The development of the heterogeneous mechanism takes into account the results from mechanistic studies reported in the literature [28-37]. Despite the many studies carried out on this subject, the exact nature of the active sites on La_2O_3 remains unclear. Yang et al. suggested that O^{2-} ions could be the active site for methane activation [38]. On the other hand for Hutchings et al. [39], the formation of CH_3. radicals is due to the O^- ions while O_2^{2-} lead to the formation of CH_2: radicals. Lacombe et al. [40] have identified various active sites on the

surface of lanthanum oxide: a basic site associated with an anionic vacancy which would be responsible for the dissociation of gaseous oxygen into atomic species and an unsaturated site on which methyl radical would react to be further oxidized into CO_2. In summary, there are at least two types of active sites on the La_2O_3 surface [41].

In our mechanism, the two types of active sites considered are: a reduced site (s) and an oxygenated site O(s). Experimental studies of oxygen chemisorption [42] have shown that this reaction occurs with dissociation of a diatomic O_2 molecule to form two active atomic oxygen centres according to the following reaction:

$$O_2(s) + s \rightarrow 2\ O(s)$$

$$2\ O(s) \rightarrow O_2(s) + s$$

In these elementary reactions s represents a surface site and O(s) the atom O adsorbed on the surface of the La_2O_3 crystal.

The heterogeneous mechanism was written systematically by considering the possible reactions between these two sites and the major reaction products and free radicals. These reactions were written according to the Eley-Rideal formalism involving the reactions between a gas phase molecule and an active site. For example, methane can react according to:

$$CH_4 + O(s) \rightarrow CH_3. + OH(s)$$

$$CH_4 + s \rightarrow CH_3. + H(s)$$

The hydroxylated sites and hydrogenated sites can react according to the Langmuir-Hinshelwood formalism leading to the formation of hydrogen and water via surface steps:

$$H(s) + H(s) \rightarrow H_2 + 2s$$

$$OH(s) + H(s) \rightarrow H_2O + 2s$$

$$2OH(s) \rightarrow O(s) + H_2O + s$$

Finally, the heterogeneous mechanism is composed of 33 direct elementary steps involving 9 surface species (Table 2).

	Réactions	A (mol, cm^2, s)	E($cal.mol^{-1}$)
1	$O_2 + s \rightarrow O_2(s)$	$1.8\ 10^7$	1500
2	$O_2(s) \rightarrow O_2 + s$	$2{,}3\ 10^{12}$	45000
3	$O_2(s) + s \rightarrow 2O(s)$	$1.2\ 10^{23}$	25000
4	$2O(s) \rightarrow O_2(s) + s$	$3.3\ 10^{23}$	33000
5	$CH_4 + O(s) \rightarrow CH_3\cdot + OH(s)$	$7.5\ 10^8$	8840
6	$C_2H_6 + O(s) \rightarrow C_2H_5\cdot + OH(s)$	$9.5\ 10^9$	3000
7	$CO + O(s) \rightarrow CO_2 + s$	$4.7\ 10^9$	0
8	$CO_2 + s \rightarrow CO_2(s)$	$6.2\ 10^8$	0
9	$CO_2(s) \rightarrow CO_2 + s$	$2.3\ 10^{13}$	43580
10	$C_2H_4 + O(s) \rightarrow C_2H_3\cdot + OH(s)$	$5.5\ 10^8$	3000
11	$C_2H_5\cdot + O(s) \rightarrow C_2H_4 + OH(s)$	$5.5\ 10^7$	0
12	$C_3H_7 + O(s) \rightarrow C_3H_6 + OH(s)$	$6.1\ 10^7$	0
13	$2OH(s) \rightarrow O(s) + H_2O + s$	$1.3\ 10^{23}$	2400
14	$CH_3\cdot + O(s) \rightarrow CH_2\cdot + OH(s)$	$1.9\ 10^9$	2800
15	$CH_2\cdot + O(s) \rightarrow CH\cdot + OH(s)$	$3.6\ 10^{11}$	11900
16	$CH\cdot + O(s) \rightarrow C + OH(s)$	$8.9\ 10^8$	4700
17	$C + O(s) \rightarrow CO + s$	$1.1\ 10^{11}$	0
18	$CH_3\cdot + O(s) \rightarrow CH_3O(s)$	$9.9\ 10^8$	600
19	$CH_3O(s) + O(s) \rightarrow HCHO + OH(s) + s$	$1.2\ 10^{23}$	0
20	$HCHO + O(s) \rightarrow CHO. + OH(s)$	$3.4\ 10^7$	3000
21	$CHO\cdot + O(s) \rightarrow CO + OH(s)$	$6.9\ 10^7$	410
22	$C_2H_5\cdot + O(s) \rightarrow C_2H_5O(s)$	$1.0\ 10^9$	600
23	$C_2H_5O(s) + O(s) \rightarrow CH_3CHO + OH(s) + s$	$6.6\ 10^{21}$	0
24	$CH_4 + s \rightarrow CH_3\cdot + H(s)$	$8.5\ 10^7$	9850
25	$C_2H_6 + s \rightarrow C_2H_5\cdot + H(s)$	$9.8\ 10^7$	5000
26	$C_2H_4 + s \rightarrow C_2H_3\cdot + H(s)$	$1.9\ 10^7$	5000
27	$H\cdot + s \rightarrow H(s)$	$9.6\ 10^{12}$	0
28	$OH(s) + H(s) \rightarrow H_2O + 2s$	$1.0\ 10^{24}$	0
29	$H(s) + H(s) \rightarrow H_2 + 2s$	$1.3\ 10^{23}$	0
30	$H_2 + 2s \rightarrow 2H(s)$	$6.1\ 10^{16}$	0
31	$H_2 + O(s) \rightarrow OH(s) + H\cdot$	$1.0\ 10^{10}$	0
32	$C + O(s) \rightarrow CO(s)$	$1.1\ 10^{11}$	0
33	$CO(s) + O(s) \rightarrow CO_2(s) + s$	$1.1\ 10^{23}$	0

Table 2. Kinetic parameters of surface reactions in oxidation of methane (s symbolizes surface site and (s) adsorbed species).

To carry out the simulations, it is necessary to calculate the kinetics parameters of this heterogeneous mechanism. There are few models involving a detailed mechanism composed of elementary steps and with estimation of the kinetics parameters. We can quote for example Deutschmann [43], Sinev [44] and Gent University [45, 46]. In our study, pre-exponential factor of elementary steps are calculated by methods derivate from Benson's techniques [47] whereas activation energies are chosen in first approximation by analogy with reactions in gas phase. Simulations were performed using the Chemkin® and Surface Chemkin® software packages in a CSTR reactor [48,49]. The simulations were performed by simultaneously compiling the homogeneous and the heterogeneous sub-mechanisms so that the possible coupling could be taken into account. It should be noted that these methods give only an approximation of the initial numerical value of parameters, usually unknown, which must be adjusted during the optimization from experimental results.

3.2.2. Pre-exponential factor

The pre-exponential factor is calculated by using partition functions of gas molecule and activated complex. For the following reaction:

$$A + B(s) \rightarrow AB^{\neq} \rightarrow \text{Products}$$

where A is a gas molecule, B(s) a surface species and $AB^{\neq}$ the activated complex, the pre-exponential factor is calculated by the following equation:

$$A = \frac{k_B T N q^{\neq}}{h q_A q_{B(s)}} \qquad (1)$$

In Eq. (1), k_B is the Boltzmann constant ($1.38\ 10^{-23}$ J.K^{-1}), N the Avogadro constant ($6.022\ 10^{23}$ mol^{-1}), T the temperature, h the Planck constant ($6.6262\ 10^{-34}$ J.s.) and q_A, $q_{B(s)}$, $q^{\neq}$ are the partition functions of A, B(s) and the activated complex. The difference between the degrees of freedom of B(s) and $AB^{\neq}$ is mainly due to the vibrations of the molecule A in the

configuration of the activated complex. Indeed, B(s) and $AB^{\neq}$ are adsorbed species and have no rotational or translational degrees of freedom. So, to simplify the calculation, we suppose than the difference between partition function of B(s) and $AB^{\neq}$ is only due to the vibrational component of the activated complex $q^{\neq}_{v}$. Then the following expression is obtained:

$$A = \frac{k_B T N q^{\neq}_{v}}{h q_A} \qquad (2)$$

The partition function of a molecule or a radical is the product of a translational partition function q_t, an external rotational partition function q_r, a vibrational partition function q_v and an electronic partition function q_e. These partition functions can be calculated by the Eq. (3).

$$q_t = \frac{(2\pi m k_B T)^{3/2}}{h^3}$$

$$q_r^{3D} = \frac{\pi^{1/2}}{\sigma_{ext}}\left(\frac{8\pi^2 k_B T}{h^2}\right)^{3/2} R^{1/2} \quad \text{or} \quad q_r^{2D} = \frac{8\pi^2 I k_B T}{\sigma_{ext} h^2}$$

$$q_v = \prod_i q_{v,i} \quad \text{and} \quad q_{v,i} = \frac{1}{1-\exp\left(\frac{-1.44\omega_i}{T}\right)}$$

$$q_e = 2s+1 \qquad (3)$$

In these equations, σ_{ext} is the external symmetry number, m (kg) the mass of the atom, s the spin and ω_i (cm^{-1}) the frequency of the tabulated vibration.

The selection of the formula for calculating the rotational partition function depends on the molecule considered. A linear molecule only possesses two rotational degrees of freedom. The two moments of inertia about the two axes of rotation are equal to I ($kg.m^2$). In this case, the rotational partition function is q_r^{2D}. However, there are 3 rotational degrees of freedom in a non-linear molecule and the calculation of the partition function q_r^{3D} use the product of the moments of inertia: D ($kg^3.m^6$). For easier use, these formulas can be rewritten:

$$q_t = 1.88\,10^{26}(MT)^{3/2} \qquad (1)$$

$$q_r^{3D} = 1.48\,10^{-2}\frac{D^{1/2}T^{3/2}}{\sigma_{ext}} \quad \text{or} \quad q_r^{2D} = 4.12\,10^{-2}\frac{IT}{\sigma_{ext}} \qquad (2)$$

In the first expression the unit of q_t is m^{-3} and M is the molar mass ($g.mol^{-1}$). In the second expression, the unit of D is $amu^3.Å^6$ and that of I is $amu.Å^2$.

3.2.3. Activation energy

The activation energy is the most difficult parameter to calculate, especially for surface reactions, because it depends on the nature of the adsorption site. Since these values are generally intended to be optimized by simulation of the experimental results, two simple methods of estimation depending on the type of reaction involved are proposed. For the adsorption/desorption reactions, the activation energy is calculated from the experimental value of adsorption enthalpy obtained from the literature. The activation energy of the other elementary surface reactions can be assumed in first estimate to be the same as the equivalent gas-phase reaction.

For example, the CO_2 adsorption – desorption can be represented by the following reactions: (3) $CO_2 + s \rightarrow CO_2(s)$

(-3) $CO_2(s) \rightarrow CO_2 + s$

The activation energy of the CO_2 adsorption is low; so the activation energy of the step (3) is supposed to be equal to 0. The adsorption enthalpy of CO_2 on the surface can be found in the literature; the adsorption enthalpy of CO_2 on La_2O_3/CaO catalyst [50] is about:

$-\Delta H_{ads,\,CO2} = 44 \pm 7\ kcal.mol^{-1} = E_{-3}$.

For the other types of surface reactions, the activation energy can be chosen, by analogy with gas phase reactions. The Eley-Rideal reaction of an ethane molecule with the surface of the catalyst: $C_2H_6 + s \rightarrow C_2H_5. + H(s)$ may be represented by the following homogeneous reaction: C_2H_6 + alkyl. $\rightarrow$ $C_2H_5.$ + alkane

We can use, for example, the reaction: $C_2H_6 + CH_3. \rightarrow C_2H_5. + CH_4$

The activation energy of this gas phase reaction [51] is: 5800 cal.mol^{-1}. At a first approximation, this value for the activation energy of the surface reaction can be used. The activation energy depends on the catalyst surface and these activation energy values can only be considered as a starting point for the simulation. Finally, a hetero-homogeneous mechanism composed of many elementary steps and their kinetic constants (A and E) was obtained.

3.3 Sensitivity analysis

For all the reactions studied, a flow consumption analysis or a sensitivity analysis can be realized to better understand the reaction and to find optimal conditions. To determine the most sensitive reactions involved in the mechanism, a sensitivity analysis was performed for each of the three reactions. The analysis was performed for major products. Figures 18 and 19 show sensitivity analysis for surface reactions for OCM and POM. The first order sensitivity coefficient for species n and reaction i was defined according to:

$$S_{i,n} = \frac{k_i}{dk_i}\frac{dx_n}{x_n} \qquad (5)$$

where k_i is the kinetic constant of reaction i and x_n is the molar fraction of species n. The higher the $S_{i,n}$ coefficient is, the more sensitive against species n the reaction i is. Moreover, a positive sensitivity coefficient $S_{i,n}$ means that an increase of the kinetic constant k_i leads to an increase of the concentration of species n. Some reactions have sensitivity coefficients lower than $|0.01|$ and can be considered negligible. Table 3 shows the final surface mechanism in which only the most important elementary reactions are present. This simplified mechanism consists of 17 elementary reactions and gives the same result as the complete mechanism with an error of less than 1%.

	Réactions	A_{fitted} (mol, cm^2, s)	E_{fitted} ($cal.mol^{-1}$)
1	$O_2 + s \rightarrow O_2(s)$	$6.0\ 10^7$	5000
2	$O_2(s) \rightarrow O_2 + s$	$2{,}3\ 10^{12}$	38000
3	$O_2(s) + s \rightarrow 2O(s)$	$2.3\ 10^{23}$	25000
4	$2O(s) \rightarrow O_2(s) + s$	$3.3\ 10^{23}$	33000
5	$CH_4 + O(s) \rightarrow CH_3\cdot + OH(s)$	$3.0\ 10^8$	8840
6	$C_2H_6 + O(s) \rightarrow C_2H_5\cdot + OH(s)$	$8.7\ 10^9$	3000
7	$CO + O(s) \rightarrow CO_2 + s$	$8.3\ 10^8$	0
10	$C_2H_4 + O(s) \rightarrow C_2H_3\cdot + OH(s)$	$1.1\ 10^{10}$	3000
13	$2OH(s) \rightarrow O(s) + H_2O + s$	$3.0\ 10^{23}$	2400
24	$CH_4 + s \rightarrow CH_3\cdot + H(s)$	$8.5\ 10^7$	9850
25	$C_2H_6 + s \rightarrow C_2H_5\cdot + H(s)$	$9.8\ 10^7$	5000
26	$C_2H_4 + s \rightarrow C_2H_3\cdot + H(s)$	$1.9\ 10^7$	5000
27	$H\cdot + s \rightarrow H(s)$	$9.6\ 10^{12}$	0
28	$OH(s) + H(s) \rightarrow H_2O + 2s$	$1.0\ 10^{24}$	0
29	$H(s) + H(s) \rightarrow H_2 + 2s$	$4.0\ 10^{23}$	0
30	$H_2 + 2s \rightarrow 2H(s)$	$6.1\ 10^{16}$	0
31	$H_2 + O(s) \rightarrow OH(s) + H\cdot$	$2.0\ 10^8$	0

Table 3. Simplified surface mechanism of methane oxidation [s symbolizes surface site and (s) adsorbed species].

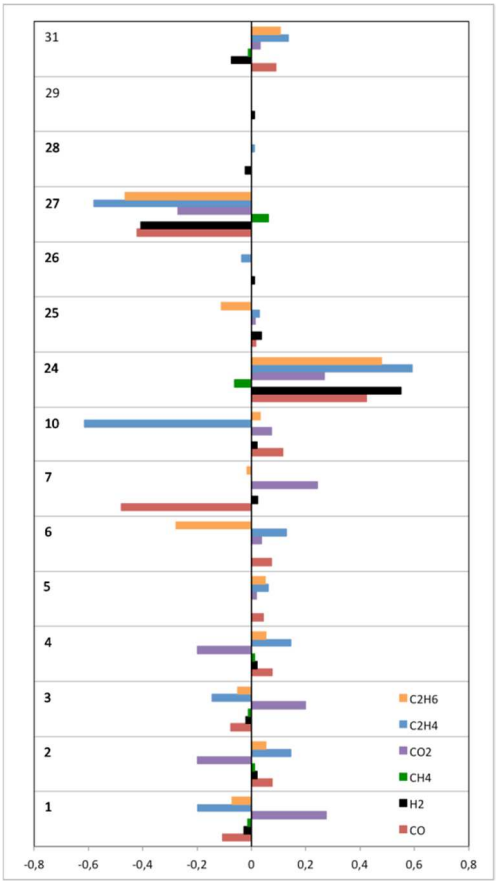

Figure 18. Sensitivity analysis of surface reactions for POM at 1123 K

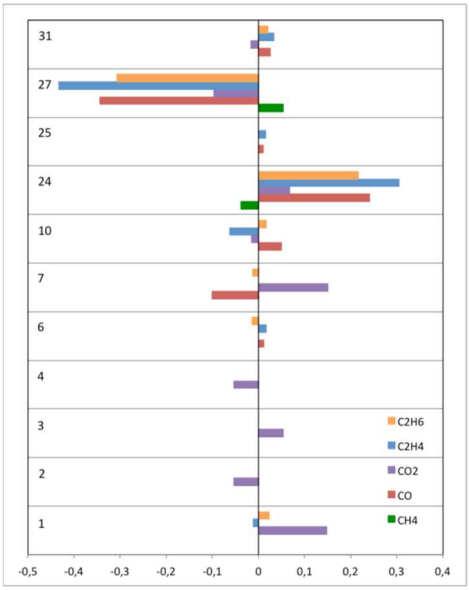

Figure 19. Sensitivity analysis of surface reactions for OCM at 1173 K

4- RESULTS AND DISCUSSION

For the three reactions of OCM, POM and HOM, the experimental curves of reactant consumption and product formation as a function of residence time were simulated. The kinetic parameters of the homogeneous reactions provide from literature [52-60] or are calculated by the Kingas [61] software (Table 1). The kinetic parameters of heterogeneous reactions are estimated using the methodology described here (Table 2) and modified to fit the model to the experimental results (Table 3). This unified hetero-homogeneous mechanism is used for the simulation of the three reactions.

4.1 Homogeneous oxidation of methane

Homogeneous oxidation of methane doesn't have a real industrial interest because of the stability of the methane molecule. However, the mechanism of this reaction is essential to represent the reactions of OCM and POM. Therefore, we have studied this reaction experimentally over a large temperature range (1083K to 1148 K) in order to determine its reaction mechanism. Figure 1 to 6 show the molar fraction of CH_4, C_2H_4, C_2H_6, CO, CO_2 and H_2 versus residence time. The ratio CH_4/O_2 was fixed to 2. The simulation very well reproduces the conversion of CH_4 and the production of the most important products.

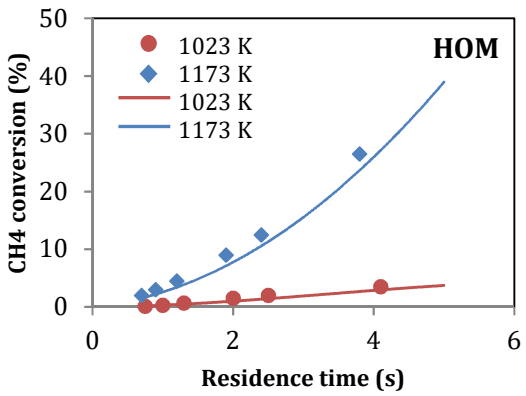

Fig.1. Conversion of CH_4 versus residence time. Comparison between experiment (symbol) and simulation (line).

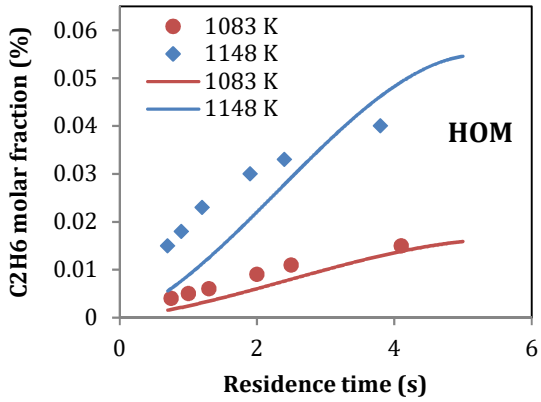

Fig.2. Molar fraction of C_2H_6 versus residence time. Comparison between experiment (symbol) and simulation (line).

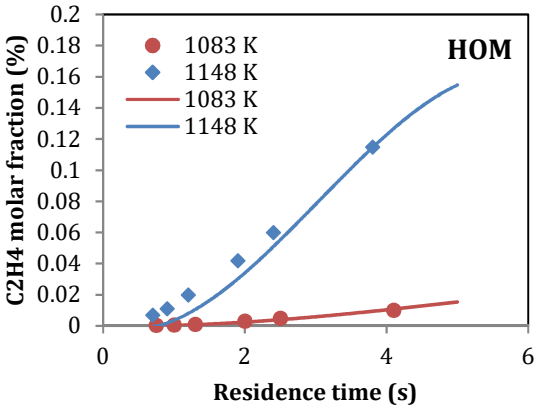

1

Fig.3. Molar fraction of C_2H_4 versus residence time. Comparison between experiment (symbol) and simulation (line).

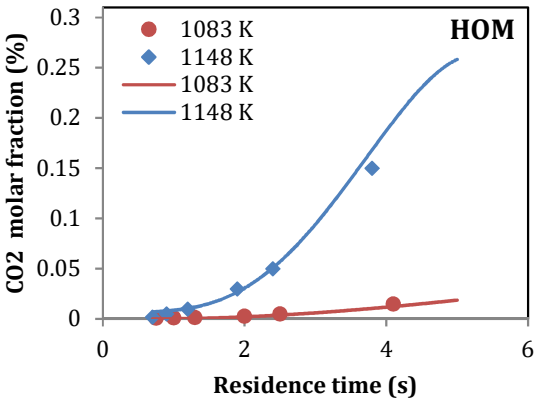

Fig.4. Molar fraction of CO_2 versus residence time. Comparison between experiment (symbol) and simulation (line).

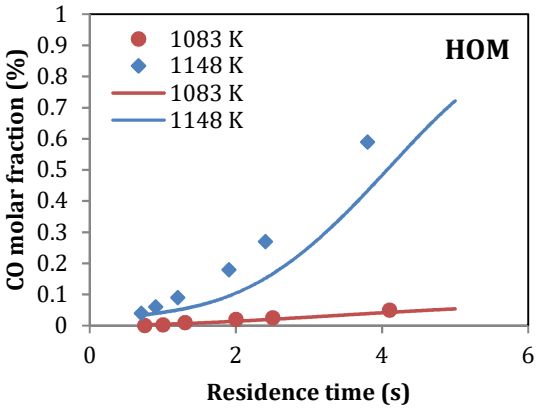

2

Fig.5. Molar fraction of CO versus residence time. Comparison between experiment (symbol) and simulation (line).

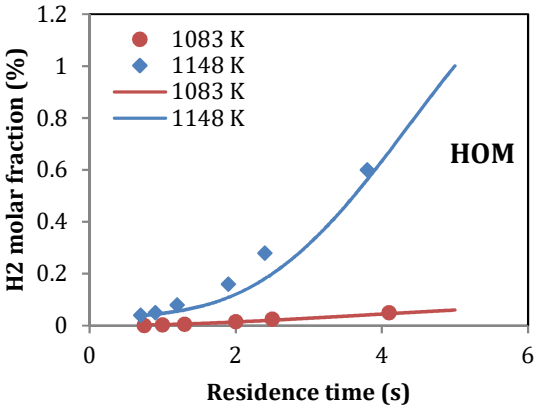

Fig.6. Molar fraction of H_2 versus residence time. Comparison between experiment (symbol) and simulation (line).

3 ## 4.2 Partial oxidation of methane

4 Among the proposed methods for the production of hydrogen, the partial oxidation of
5 methane has many advantages: the reaction is exothermic and it may be carried out in
6 autothermal conditions. This reaction produces syngas: $CH_4 + ½\,O_2 = CO + 2\,H_2$
7 The reaction was studied at various temperatures between 973K and 1123K over La_2O_3
8 catalyst. Like for HOM, the ratio CH_4/O_2 was 2. The concentration of sites over the surface L

was unknown. So we used an average value of L = 910^{-11} mol.cm^{-2} as the starting point. L was thus considered as an adjustable parameter and the value used after adjustment was finally:

L = 2.810^{-11} mol.cm^{-2}. Figure 7 to 12 show the variation of the molar fraction of CH_4, C_2H_4, C_2H_6, CO, CO_2 and H_2 according to the residence time at two temperatures. A good agreement between the experimental and theoretical results can be observed.

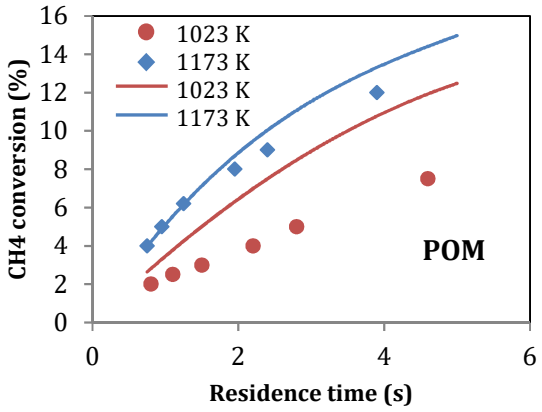

Fig.7. Conversion of CH_4 versus residence time. Comparison between experiment (symbol) and simulation (line).

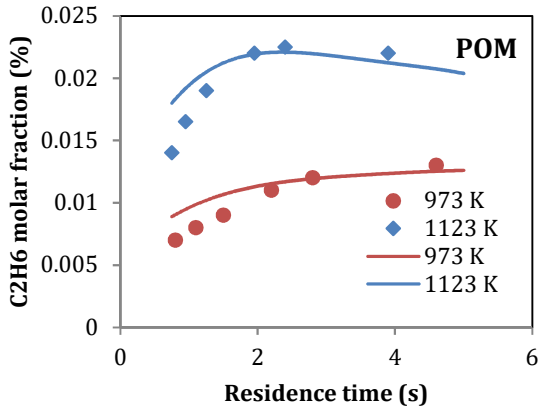

Fig.8. Molar fraction of C_2H_6 versus residence time. Comparison between experiment (symbol) and simulation (line).

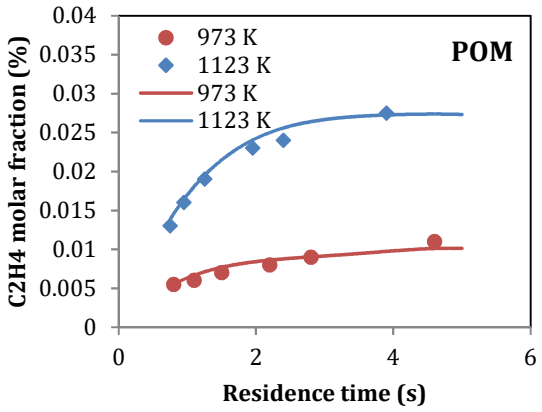

Fig.9. Molar fraction of C_2H_4 versus residence time. Comparison between experiment (symbol) and simulation (line).

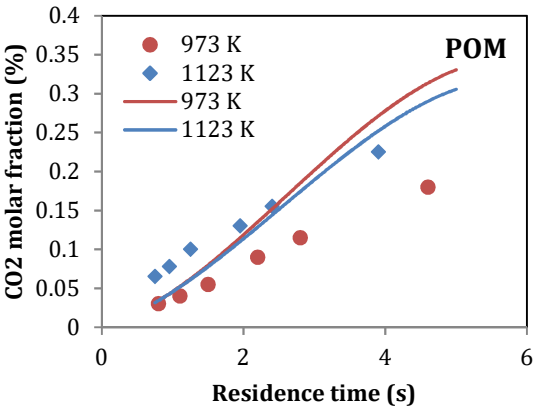

Fig.10. Molar fraction of CO_2 versus residence time. Comparison between experiment (symbol) and simulation (line).

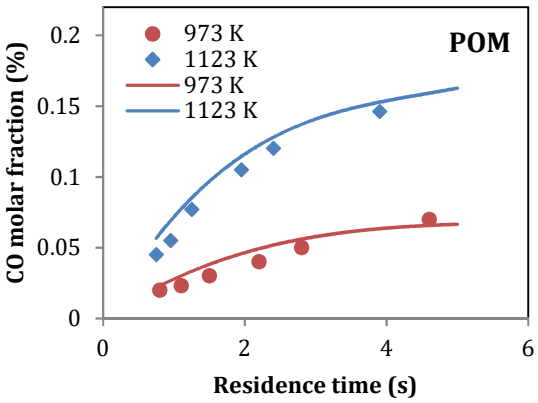

1

Fig.11. Molar fraction of CO versus residence time. Comparison between experiment (symbol) and simulation (line).

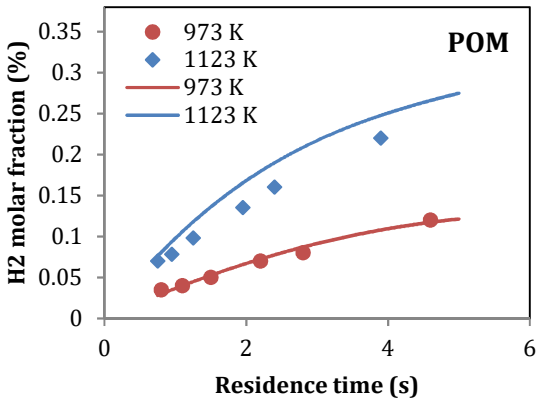

Fig.12. Molar fraction of H_2 versus residence time. Comparison between experiment (symbol) and simulation (line).

2 ## 4.3 Oxidative coupling of methane

3 The reaction of oxidative coupling of methane has been investigated in a large number
4 of laboratories because its development should have led to a direct process to obtain more
5 valuable hydrocarbons such as ethylene for the chemical industry:

6 $$2\,CH_4 + 1/2O_2 = C_2H_4 + 2H_2O$$

7 This reaction was studied between 1023K and 1173K over La_2O_3 catalyst with a CH_4/O_2 ratio
8 of 5. Like for POM, the concentration of sites over the surface was $L = 910^{-11}$ mol.cm^{-2} as the
9 starting point and the value used after adjustment was $L = 510^{-11}$ mol.cm^{-2}. Figure 13 to 17
10 shows the molar fraction of CH_4, C_2H_4, C_2H_6, CO and CO_2 according to the residence time.
11 Although the kinetic parameters were only slightly modified the agreement between the
12 theoretical curves and the experimental points was correct. Therefore the hetero-
13 homogeneous mechanism was validated in the experimental conditions.

14

1

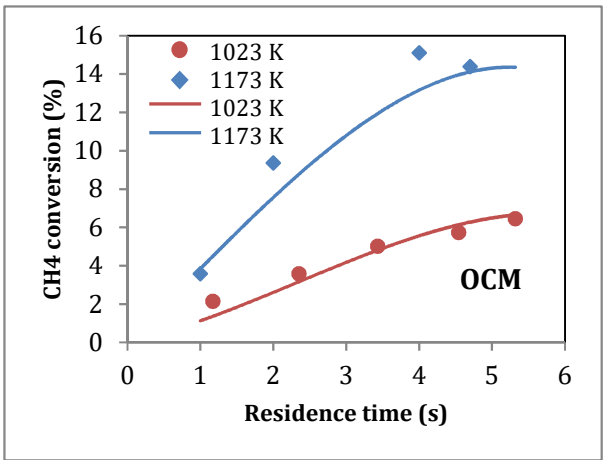

Fig.13. Conversion of CH_4 versus residence time. Comparison between experiment (symbol) and simulation (line).

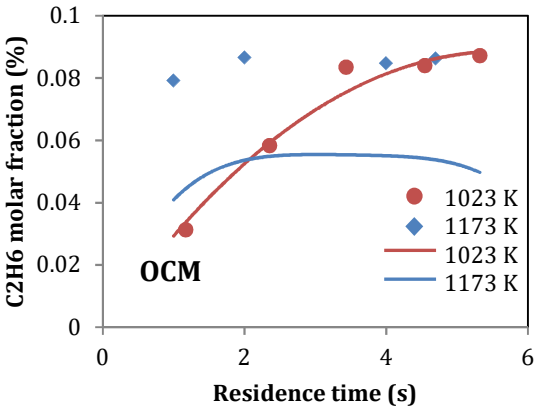

Fig.14. Molar fraction of C_2H_6 versus residence time. Comparison between experiment (symbol) and simulation (line).

2

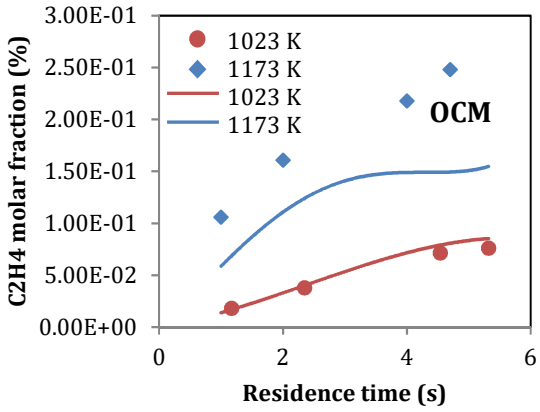

Fig.14. Molar fraction of C_2H_4 versus residence time. Comparison between experiment (symbol) and simulation (line).

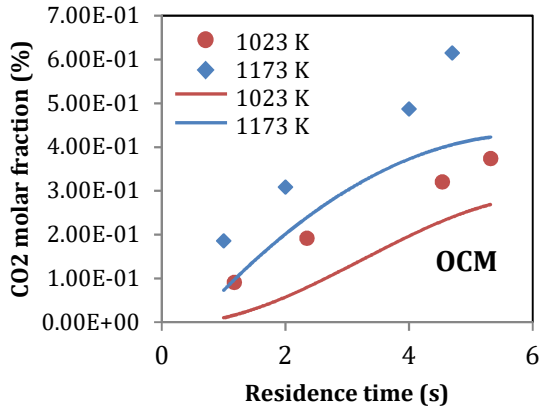

Fig.16. Molar fraction of CO_2 versus residence time. Comparison between experiment (symbol) and simulation (line).

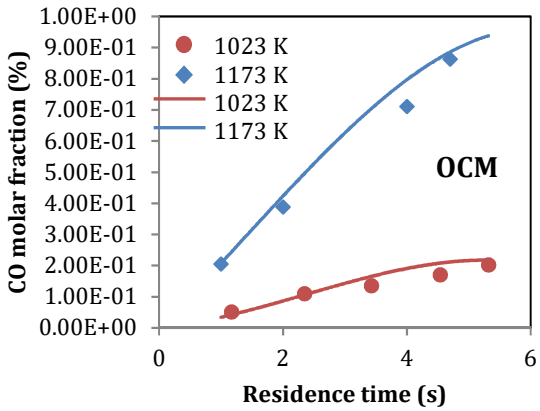

Fig.17. Molar fraction of CO versus residence time. Comparison between experiment (symbol) and simulation (line).

4.4 Comparison of the three reactions

A simplification of the general mechanism can be represented according to figure 20. The mechanism of oxidation of methane comprises two distinct reaction pathways: an oxidative route and a non-oxidative route.

The initiation of the oxidation of methane forms CH_3. radicals (reaction 1). In the case of HOM, the activation occurs by reaction between CH_4 and a gas phase radical while in OCM and POM the initiation takes place mainly on the catalyst by reactions involving surface species.

$CH_4 + O(s) \rightarrow CH_3. + OH(s)$

$CH_4 + s \rightarrow CH_3. + H(s)$

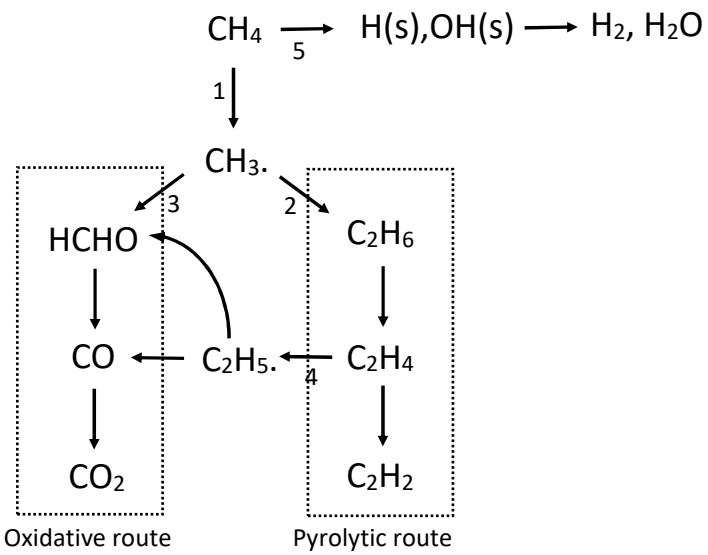

Fig.20. Schematic representation of the mechanism

Heterogeneous initiations represent 80% of the methane activation in the case of POM and 100% in the case of OCM. The main effect of the catalyst is the generation of free radicals.

Then, the CH_3. radicals can react according to the pyrolytic route (reaction 2) to form hydrocarbons or the oxidative route (reaction 3) to form oxygenated compounds. The pyrolytic route and therefore the formation of hydrocarbons is favored when the concentration of oxygen is low, which is the case for OCM. When the conversion is high, an oxidative step appears (reaction 4). This step decreases the concentration of C_2H_4 and may explain why the yield of hydrocarbons in OCM does not exceed 22% to 27% for all catalysts tested, like reported by numerous authors.

In POM and HOM, the oxygen concentration favors the oxidative pathway. However, lanthanum oxide is an excellent generator of free radical. Thus, in POM, the catalyst more easily generates radicals by reactions between CH_4 and surface species and therefore

accelerates the reaction. In addition, a new source of H_2 formed by heterogeneous reactions (reaction 5) appears on lanthanum oxide, which increases the yield of H_2 in POM.

5. CONCLUSION

The study of catalytic oxidations of methane has met with renewed interest in the past 10 years due to the discovery of new natural gas fields and the rising price of oil. These catalytic reactions are carried out at high temperature and thus comport a homogeneous and heterogeneous part, which make their mechanism more complex. This reaction mechanism is essential for the development of industrial processes. We have therefore developed a reaction mechanism that allows representing, at the same time, three methane oxidation reactions: homogeneous oxidation, partial oxidation and oxidative coupling. The homogeneous mechanism may be found in the literature or determined from an automatic generator of mechanism. The heterogeneous mechanism was written following the Eley-Rideal and Langmuir-Hinshelwood formalisms. The pre-exponential factor was determined by methods derived from Benson's technics whereas the activation energy was chosen, in a first time, by analogy with gas phase reactions. Finally, the mechanism used for the simulation give good results although the values of the rate constants were only slightly modified. Thanks to the sensitivity analysis, the heterogeneous mechanism has been simplified and contains only 17 elementary reactions.

NOMENCLATURE

k_i: Rate constant for elementary step i

A: Arrhenius preexponential factor

E: Activation energy ($cal.mol^{-1}$)

T: temperature (K)

k_B: Bolzmann constant: 1.381 10^{-23} $J.K^{-1}$

h: Planck constant : 6.6262 10^{-34} J.s.

N: Avogadro number: 6,022 10^{23}

q_i: total partition function for species i (m^{-3})

q_{iv}: vibrational partition function for species i

q_{ir}: rotational partition function for species i

q_{it}: translational partition function for species i (m^{-3})

q_{ie}: electronic partition function for species i

$\neq$: in relation with the activated complex

m: molecule mass (kg)

M: molar mass (g. mol^{-1})

s: spin quantic number

σ_{ext}: external symmetry number

σ_{int}: internal symmetry number

I: moment of inertia (amu. A^2 or kg. m^2)

I_{red}: reduced moment of inertia (amu. A^2)

ω: frequency of vibration (cm^{-1})

D: product of the moments of inertia ($amu^3.Å^6$ or kg^3. m^6)

$\Delta H_{ads,i}$: heat of adsorption for species i ($cal.mol^{-1}$)

x_n: molar fraction for species n

$S_{i,n}$: sensibility coefficient of reactions i for species n

BIBLIOGRAPHY

[1] BP statistical review of world energy **2020**.

[2] Keller GE, Bhasin MM. Synthesis of Ethylene via Oxidative Coupling of Methane I. Determination of Active Catalysts, J. Catal. **1982**, 73, 9-19.

[3] Choudhary VR, Mulla SAR, Uphade BS. Oxidative coupling of methane over alkaline earth oxides deposited on commercial support precoated with rare earth oxides, Fuel **1999**, 78, 427-437.

[4] Rostrup-Nielsen JR, Christiansen LJ, Bak Hansen JH. Activity of steam reforming catalysts: role and assessment, Appl. Catal. **1988**, 43(2), 287.

[5] Rostrup-Nielsen JR, Sehested J, Nørskov JK. Hydrogen and Synthesis Gas by Steam and CO_2 Reforming, Adv. Catal. **2002**, 47, 65.

[6] Corbo P, Migliardini F. Hydrogen production by catalytic partial oxidation of methane and propane on Ni and Pt catalysts, Int. J. Hydrogen Energy **2006**, 32, 55-66.

[7] Requies J, Barrio VL, Cambra JF, Güemez MB, Arias PL, La Parola V, Pena MA, Fierro JLG. Effect of redox additives over Ni/Al_2O_3 catalysts on syngas production via methane catalytic partial oxidation, Fuel **2008**, 87, 3223-3231.

[8] Subramanian R, Panuccio GJ, Krummenacher JJ, Lee IC, Schmidt LD. Catalytic partial oxidation of higher hydrocarbons: reactivities and selectivities of mixtures, Chem. Eng. Sci. **2004**, 59, 5501.

[9] Bistolfi M, Fornasari G, Molinari M, Palmery S, Dente M, Ranzi E. Kinetic Model for methane oxidative coupling reactors, Chem. Eng. Sci. **1992**, 47, 2647.

[10] Driscoll DJ, Lunsford JH. Gas-Phase Radical Formation during the Reaction of Methane, Ethane, Ethylene and Propylene over selected Oxide Catalysts, J. Phys. Chem. **1985**, 89, 4415.

[11] Driscoll DJ, Martir W, Wang J, Lunsford, JH. Formation of Gas Phase Methyl Radicals over MgO, J. Am. Soc. **1985**, 107, 58.

[12] Sinev MY. Kinetic modeling of heterogeneous-homogeneous radical processes of the partial oxidation of low paraffins, Catal. Today **1995**, 24, 389.

[13] Baerns M, Buyevskaya OV, Mleczko L, Wolf D. Catalytic partial oxidation of methane to synthesis gas - catalysis and reaction engineering, Stud. Surf. Sci. Catal. **1997**, 107.

[14] Deutschmann O, Schmidt LD. Modeling the partial oxidation of methane in a short-contact-time reactor, AIChE J. **1998**, 44, 2465.

[15] Goralski CT, O'Connor RP, Schmidt LD. Modeling homogeneous and heterogeneous chemistry in the production of syngas from methane, Chem. Eng. Sci. **2000**, 55, 1357.

[16] Fleys M, Simon Y, Marquaire PM. Discussion on the oxidative and the pyrolysis routes of the CH_3 radicals in the partial oxidation of methane over La_2O_3, J. Anal. Appl. Pyrol. **2007**c, 79, 259.

[17] Thybaut JW, Sun J, Olivier L, Van Veen AC, Mirodatos C, Marin GB. Catalyst design based on microkinetic models: oxidative coupling of methane, Catal. Today **2011**, 159, 29.

[18] Hickman DA, Schmidt LD. Production of syngas by direct catalytic oxidation of methane, Science **1993**, 259, 343.

[19] Vlachos DG. Homogeneous-heterogeneous oxidation reactions over platinum and inert surfaces, Chem. Eng. Sci. **1996**, 51, 2429.

[20] Fleys M, Simon Y, Marquaire PM. Detailed kinetic study of the partial oxidation of methane over La_2O_3 catalyst. Part 2: mechanism, Ind. Eng. Chem. Res. **2007**a, 46, 1069 - 1078.

[21] Fleys M, Shan W, Simon Y, Marquaire PM. Detailed kinetic study of the partial oxidation of methane over La_2O_3 catalyst. Part 1: Experimental results, Ind. Eng. Chem. Res. **2007**b, 46, 1063.

[22] Fleys M, Simon Y, Swierczynski D, Kiennemann A, Marquaire PM. Investigation of the reaction of partial oxidation of methane over Ni/La_2O_3 catalyst, Energy & Fuels **2006**, 20, 2321.

[23] Simon Y, Baronnet F, Marquaire PM. Kinetic modeling of the oxidative coupling of methane, Ind. Eng. Chem. Res. **2007**, 46, 1914–1922.

[24] Barbé P, Li YD, Marquaire PM, Côme GM, Baronnet F. Competition between the gas and surface reactions for the oxidative coupling of methane. 1. "Non-isothermal" results in catalytic jet-stirred reactor, Catal. Today **1994**, 21, 409.

[25] Barbé P, Li YD, Marquaire PM, Côme GM, Baronnet F. A new "catalytic jet-stirred reactor" Application to the study of the oxidative coupling of methane, Oxid. Commun **1996**, 19, 173.

[26] Hognon C, Simon Y, Marquaire PM, Courson C and Kienneman A. Hydrogen production by catalytic partial oxidation of propane over CeO_2, Chem. Eng. Sc. **2018**, 181, 46-57.

[27] Warth V, Battin-Leclerc F, Fournet R, Glaude PA, Côme GM, Scacchi G. Computer based generation of reaction mechanisms for gas-phase oxidation, Comput. Chem. **2000**, 24, 541.

[28] McCarty JG. Methane Conversion by Oxidative Processes, Wolf EE, Ed. Van Nostrand Reinhold, **1992** New York.

[29] Martin GA, Mirodatos C. Surface chemistry in the oxidative coupling of methane. Fuel Process. Technol. **1995**, 42, 179.

[30] Lacombe S, Durjanova Z, Mleczko L, Mirodatos C. Kinetic modelling of the oxidative coupling of methane over lanthanum oxide in connection with mechanistic studies, Chem. Eng. Technol. **1995**, 42, 216.

[31] Couwenberg PM, Chen Q, Marin GB. Kinetics of a gas- phase chain reaction catalysed by a solid: The oxidative coupling of methane over Li/MgO-based catalysts, Ind. Eng. Chem. Res. **1996**, 35, 3999.

[32] Wolf D, Slinko M, Baerns M, Kurkina E. Kinetic simulations of surface processes of the oxidative coupling of methane over a basic oxide catalyst, Appl. Catal. A **1998**, 166, 47.

[33] Coulter K, Goodman DW. The role of carbon dioxide in the oxidative dimerization of methane over Li/MgO, Catal. Lett. **1993**, 20, 169.

[34] Shi C, Xu M, Rosynek MP, Lunsford JH. Origin of kinetic isotope effects during the oxidative coupling of methane over a lithium (1+)/magnesia catalyst, J. Phys. Chem. **1993**, 97, 216.

[35] Sinev MYu, Fattakhova ZT, Lomonosov VI, Gordienko AYu. Kinetics of oxidative coupling of methane: Bridging the gap between comprehension an description, J. Nat. Gas Chem. 18, **2009**, 273-287.

[36] Karakaya C, Zhu H, Loebick C, Weissman JG, Kee RJ. A detailled reaction mechanism for oxidative coupling of methane over $Mn/Na_2WO_4/SiO_2$ catalyst for non-isothermal conditions, Catal. Today. **2018**, 312, 10.

[37] Beck B, Fleischer V, Arndt S, Hevia MG, Urakawa A, Hugo P, Schomäcker R, Catal. Today. **2014**, 228, 212.

[38] Yang T, Feng L, Shen S. Oxygen species on the surface of La_2O_3/CaO and its role in the oxidative coupling of methane, J. Catal. **1994**, 145, 384.

[39] Hutchings GJ, Woodhouse JR, Scurrell MS. Partial oxidation of methane over oxide catalysts. Comments on the reaction mechanism, J. Chem. Soc. Faraday Trans. **1989**, 85, 2507.

[40] Lacombe S, Geantet C, Mirodatos C. Oxidative coupling of methane over lanthana catalysts. I. Identification and role of specific active sites, J. Catal. **1994**, 151, 439.

[41] Huang S-J, Walters AB, Vannice MA. Adsorption and decomposition of NO on lanthanum oxide, J. Catal. **2000**, 192, 29.

[42] Gambo Y, Jalil AA, Triwahyono S, Abdulrasheed AA. Recent advances and future prospect in catalysts for oxidative coupling of methane to ethylene : A review, J. Ind. Eng. Chem. **2018**, 59, 218-229.

[43] Zerkle DK, Allendorf MD, Wolf M, Deutschmann O. Understanding homogeneous and heterogeneous contributions to the platinum-catalyzed partial oxidation of ethane in a short-contact-time reactor, J. Catal. **2000**, 196, 18-39.

[44] Sinev MY. Free radicals in catalytic oxidation of light alkanes: kinetic and thermochemical aspects, J. Catal. **2003**, 216, 468-476.

[45] Sun J, Thybaut JW, Marin GB. Microkinetics of methane oxidative coupling, Catal. Today **2008**, 137, 90-102.

[46] Thybaut JW, Sun J, Olivier L, Van Veen AC, Mirodatos C, Marin GB. Catalyst design based on microkinetic models: oxidative coupling of methane, Catal. Today **2011**, 159, 29.

[47] Benson SW. Thermochemical kinetics : methods for the estimation of thermochemical data and rate parameters, J. Wiley & sons, New York **1976**.

[48] Glarborg P, Kee RJ, Grcar JF, Miller JA. PSR: a Fortran program for modeling well-stirred reactors, Sandia Report, SAND86-8209 UC-4, **1990**.

[49] Coltrin ME, Kee RJ, Rupley FM, Surface Chemkin (v 4.0): a Fortran package for analyzing heterogeneous chemical kinetics at a solid surface - gas phase interface, Sandia Report, SAND90-8003C – UC-706, **1991**.

[50] Toops TJ, Walters AB, Vannice MA. The effect of CO_2 and H_2O on the kinetics of NO reduction by CH_4 over La_2O_3/γ-Al_2O_3 catalyst, J. Catal. **2003**, 214, 292-307.

[51] Baulch DL, Cobos CJ, Cox RA, Esser C, Frank P, Just T, Kerr JA, Pilling MJ, Troe J, Walker RW, Warnatz J. Evaluated kinetic data for combustion modelling, J. Phys. Chem. Ref. Data **1992**, 21, 411-429.

[52] Tsang W, Hampson RF. Chemical kinetic data base for combustion chemistry. Part I. methane and related compounds, J. Phys. Chem. Ref. Data **1986**, 15(3), 1087.

[53] Ranzi E, Sogaro A, Gaffuri P, Pennati G, Faravelli T. A wide range modelling study of methane oxidation, Comb. Sci. and Technol. **1994**, 96, 279.

[54] Cavanagh J, Cox RA, Olson G. Computer modeling of cool flames and ignition of acetaldehyde, Comb. Flame **1990**, 82, 15.

[55] Schulz G, Klotz H-D, Spangenberg H-J. Reaktionsmodell zur bruttokinetik der pyrolyse von methan im stosswellenrohr bei temperaturen von 1800 K bis 2500 K, Z. Chem. **1985**, 25, 88.

[56] Knyazev VD, Bencsura A, Stoliarov SI, Slagle IR. Kinetics of the $C_2H_3 + H_2 = H + C_2H_4$ and $CH_3 + H_2 = H + CH_4$ reactions, J. Phys. Chem. **1996**, 100, 11346.

[57] Zhang HX, Ahonkhai SI, Back MH. Rate constants for abstraction of hydrogen from benzene, toluene, and cyclopentane by methyl and ethyl radicals over the temperature range 650-770 K, Can. J. Chem. **1989**, 67, 1541.

[58] Benson SW. Oxygen Initiated Combustion: Thermochemistry and Kinetics of Unsaturated Hydrocarbons, Int. J. Chem. Kin. **1996**, 28, 665.

[59] Mahmud K, Marshall P, Fontijn A. A High-Temperature Photochemistry Kinetics Study of the Reactions of O Atoms With Acetylene From 290 to 1510 K, J. Phys. Chem. **1987**, 91, 1568.

[60] Glarborg P, Miller JA, Kee RJ. Kinetic modeling and sensitivity analysis of nitrogen oxide formation in well-stirred reactors, Comb. Flame **1986**, 65, 177.

[61] Warth V, Stef N, Glaude PA, Battin-Leclerc F, Scacchi G, Côme G-M. Computed aided design of gas-phase oxidation mechanisms: Application to the modelling of normal-butane oxidation, Comb. Flame **1998**, 114, 81-102.